Rapid Communications

Evidence for the role of the magnon energy relaxation length in the spin Seebeck effect

Arati Prakash,[1] Benedetta Flebus,[2] Jack Brangham,[1] Fengyuan Yang,[1] Yaroslav Tserkovnyak,[2] and Joseph P. Heremans[3,1,4]

[1]*Department of Physics, The Ohio State University, Columbus, Ohio 43210, USA*

[2]*Department of Physics and Astronomy, University of California, Los Angeles, California 90095, USA*

[3]*Department of Mechanical Engineering, The Ohio State University, Columbus, Ohio 43210, USA*

[4]*Department of Materials Science and Engineering, The Ohio State University, Columbus, Ohio 43210, USA*

(Received 27 June 2017; published 29 January 2018)

Temperature-dependent spin Seebeck effect data on Pt|yttrium iron garnet (YIG) ($Y_3Fe_5O_{12}$)|gallium gadolinium garnet ($Gd_3Ga_5O_{12}$) are reported for YIG films of various thicknesses. The effect is reported as a spin Seebeck resistivity (SSR), the inverse spin-Hall field divided by the heat flux, to circumvent uncertainties about temperature gradients inside the films. The SSR is a nonmonotonic function of YIG thickness. A diffusive model for magnon transport demonstrates how these data give evidence for the existence of two distinct length scales in thermal spin transport, a spin-diffusion length, and a magnon energy relaxation length.

DOI: 10.1103/PhysRevB.97.020408

Since the discovery of the (longitudinal) spin Seebeck effect (SSE) [1], much work has been done to identify the length scales involved in the phenomenon [2]. Using nonlocal detection, it has been shown that relaxation of thermal magnons in yttrium iron garnet (YIG) is governed by a spin-diffusion length λ_s, which is reported to be around 10 μm [3–5]. The latter is reported to be around 10 μm and in some studies increases to up to 70 μm at low temperatures [4,5]. This has led to a consensus that the micron-scale dependence of SSE observed in planar geometries corresponds to the generation and accumulation of the nonequilibrium magnon density gradients in the bulk. It is clear that magnon energy relaxation mechanisms by the phononic environment must be invoked generally for a complete understanding of thermal spin transport and particularly for the physics underlying the SSE. Indeed, while heaters and thermometers couple to phonons, these must in turn couple to magnons in order to give rise to the SSE in a magnon-based system, such as YIG. These relaxation processes can be parametrized by the length λ_u over which magnon-to-phonon thermalization occurs [6], and λ_u is expected to be a much smaller length scale than λ_s; a theoretical argument can be found in Ref. [7]. Several prior attempts were made to quantify λ_u. Multiparameter fits to spin Seebeck [5] and spin Peltier [8] measurements derive a value for λ_u that are up to one order of magnitude shorter than the lattice spacing of YIG (1.237 nm), indicating that the models used do not resolve the difference between magnon and phonon temperatures. Brillouin light-scattering measurements of the magnon temperature [9] also do not resolve a difference between magnon and phonon temperatures, albeit within an experimental resolution ($\pm$4 K) that is one to two orders of magnitude larger than the temperature difference across a YIG layer in a classical spin Seebeck configuration. Phonon-magnon drag has been put into evidence in previous SSE experiments [10,11], which again points to the importance of magnon-phonon interactions but do not quantify it. Therefore, other than the fits mentioned above, experimentally explicit evidence for the effect of this length scale on SSE measurements has been lacking. For completeness, we draw attention to the length scale extracted from the heat-pulse measurements in Ref. [12]. Although this length scale may be expected to be long and possibly intermediate between λ_u and λ_s, its extraction relies on the coupled heat-spin dynamics near the interface that is associated with innately transient behavior.

Previous articles on thin films using various growth techniques [13–15] have shown the SSE signal to increase with increasing YIG film thickness. In this Rapid Communication, we grow a series of Pt|YIG| gallium gadolinium garnet (GGG) heterostructures with YIG thickness varying from 10 nm to 1 μm using the same growth technique for all films. We measure the temperature-dependent spin Seebeck effect on these structures and of bulk single-crystal Pt|YIG. The spin Seebeck signal increases for film thicknesses from 10 to 250 nm and again for the bulk YIG film, but in between, the signal reaches a local maximum at a thickness of $\sim$250 nm—a detailed comparison with previous studies follows.

We explain the nonmonotonic behavior in terms of the energy-equilibration dynamics of magnons to phonons in the YIG. We implement a diffusive model for spin and heat transport in order to parametrize magnon-phonon thermal relaxation [6,7], which allows us to interpret our observations. Using typical material parameters for YIG and values for interfacial thermal conductances of the Pt|YIG|GGG heterostructure from Ref. [16], we calculate the thermally driven spin current as a function of the YIG film thickness. In our picture, a local maximum is governed by the magnon energy relaxation length, and the spin current eventually saturates at thicknesses beyond the measured magnon spin-diffusion length. Thus, the nonmonotonicity is evidence that there are two mechanisms at play, occurring on two different length scales, which define the magnonic spin Seebeck effect.

A series of YIG films with varied thicknesses (10, 40, 100, 250, 500 nm, and 1 μm) were grown epitaxially on single-crystal GGG ⟨100⟩ substrates by ultrahigh-vacuum off-axis sputtering. The growth of the 1-μm-thick film took nearly 2 days; longer growths were not technically feasible because

 ©2018 American Physical Society

the target conditions cannot be maintained stably over longer periods of growth time. Then, Pt layers of thicknesses of 6 nm were deposited at room temperature on the YIG films also by off-axis sputtering. A bulk 500-μm single-crystal YIG $\langle 100 \rangle$ substrate was obtained from Princeton Scientific so that YIG crystal orientation was controlled for all samples. Pt was deposited on this bulk crystal in the manner described for GGG. The quality of the films of all thicknesses used for SSE measurements is verified to be uniform by vibrating sample magnetometer measurements of the saturation magnetization and by measurements of the ferromagnetic resonance linewidth. The data on the films up to 250-nm thicknesses are in Refs. [17,18]. The Supplemental Material reports additional measurements of the saturation magnetization, extending the results to YIG films of 1-μm thicknesses [19].

Spin Seebeck thermopower measurements were conducted at low temperatures from 2 to 300 K on a Physical Property Measurement System by Quantum Design [20]. Although the electrical measurements are quite accurate, the measurements of the imposed temperature profile are not because this quantity must be estimated across the layer of YIG that supports magnon transport. Practical measurements obtain one of two values. First, they may obtain the temperature difference ΔT across the full Pt|YIG|GGG stack and proportion this somehow across the layers. Second, they may estimate a value for the temperature gradient ∇T from a heat flux measurement combined with a known value of thermal conductivity. Crucially, the estimates of ∇T require the knowledge of its variation across the Pt|YIG|GGG stack, which is inaccessible experimentally given the presence of interfacial thermal resistances (Pt|YIG and YIG|GGG), differences between the thermal conductivities of the different layers, and the fact that the thermal conductivity of the YIG film is not known accurately since it depends on thickness. We show in detail in the Supplemental Material [19] how these methods yield inconsistent conclusions. Particularly, the temperature dependence of the experimental results when represented as a spin Seebeck coefficient (SSC) in thermopower units (μV/K) reflects, in essence, the temperature dependence of the thermal conductivity of bulk YIG or GGG, which is dominated by phonons above 10 K [21]. Furthermore, recent work [22] systematically shows the lack of repeatability and, thus, reliability of this representation of the magnitude of the SSE.

In a proper adiabatic sample mount, the heat flux j_Q (in units of W/m^2) is unidirectional, flows entirely into the sample, and is measured reliably from the knowledge of the sample cross section and the amount of electrical power dissipated by a resistive heater. Cryostat calibrations show the heat losses to be at most 15 mW/K at 300 K, slightly less than two orders of magnitude lower than the thermal conductance of the sample so that j_Q is a well-defined experimental quantity by which we can parametrize the spin Seebeck response.

Circumventing the need to estimate ∇T, we report our data in terms of a spin Seebeck resistivity (SSR) $R_{\mathrm{SSE}} \equiv E_{\mathrm{Pt}}/j_Q$ (in units of m/A) as a function of temperature in Fig. 1. From these data, we derive the thickness dependence of the SSR over a broad temperature range, spanning 20 to 300 K in Fig. 2. The data show two features. The first is the nonmonotonic behavior of the thickness dependence of the SSR described above: The signal shows first an increase with increasing thickness up to 250 nm but is followed by a clearly resolved decrease, leading

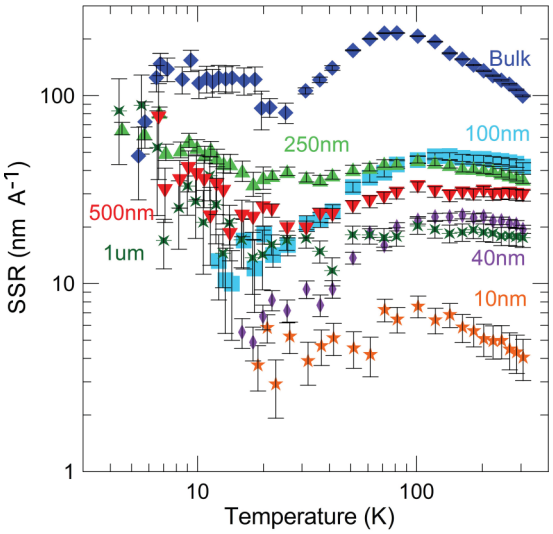

FIG. 1. Temperature dependence of the SSR for various YIG film thicknesses and bulk YIG.

to a minimum at or slightly above 1 μm. Second, although the data on bulk YIG clearly are dependent on temperature, those below 1 μm have only a weak dependence. We point out that this feature is seen best when the data are plotted as the SSR (per unit heat flux) and less so in the SSC (μV/K) [19].

These results are discussed in the context of the existing literature. Reference [13] studies thickness dependence of the SSE on two different sample sets: The results suggest a saturation of the SSE signal at 200 nm for the first set and around 10 μm for the second. Film thicknesses in the pertinent interval (between 200 nm and several microns) are not studied. The data from Ref. [13] are thus broadly consistent with the observations of Fig. 2. The nonmonotonicity appears to be absent in Ref. [14] in the relevant thickness range. However, there are rather few data points in that range, and the SSE signals are an order of magnitude lower than those presented here (in units of μV/K in the Supplemental Material [19]) so

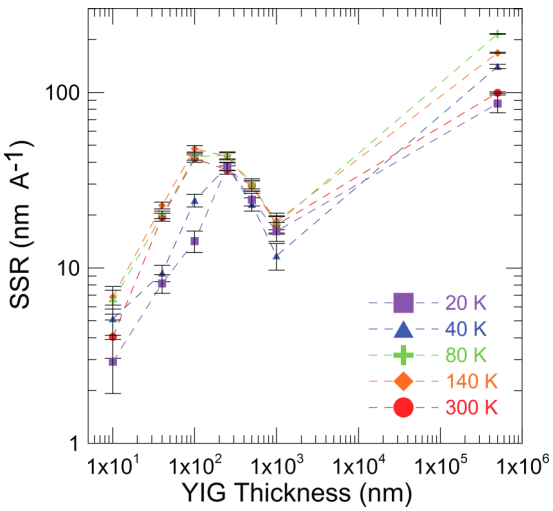

FIG. 2. Thickness dependence of the SSR at the various temperatures indicated on the graph.

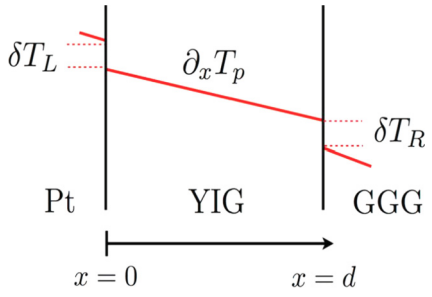

FIG. 3. Qualitative illustration of the phonon temperature profile in a Pt|YIG|GGG heterostructure.

that the amplitude falls quite close to the apparent resolution in Ref. [14]. These factors would make it difficult to resolve the local maximum reported in Fig. 2. Finally, in Ref. [15], which uses a different measurement method, the thickness dependence of the SSE voltage shows one outlying data point at 200 nm, which corresponds rather well to the observation in Fig. 2. This point also deviates from the model, which is based on only a magnon diffusion length. In fact, the discussion in Ref. [15] concludes that the local SSE may be governed by a length scale different from the magnon-diffusion length that is extracted from nonlocal signals. From this comparison to the literature, it appears that Fig. 2 offers insight to such a length scale by adding data points in the relevant YIG thickness range.

We model the experiment by considering the one-dimensional geometry shown in Fig. 3. The experimentally controlled heat flux defines the phonon temperature gradient $\partial_x T_p < 0$ in YIG. We treat phonon transport as diffusive, and we assume that the phonon temperature in the YIG T_p is not perturbed significantly by the magnons. The temperature drops at the left interface $\delta T_L = T_{p,L} - T_p(0)$ and at the right $\delta T_R = T_p(d) - T_{p,R}$, with $T_{p,L(R)}$ being the phonon temperature in Pt (GGG), can then be determined by solving the phonon heat-diffusion Eq. (16),

$$\delta T_{L(R)} = -\ell_{L(R)}\, \partial_x T_p. \tag{1}$$

Here, we have introduced the Kapitza length of the Pt(GGG)|YIG interface as $\ell_{L(R)} = \kappa_p / K_{p,L(R)}$, where κ_p is the YIG phonon thermal conductivity and $K_{p,L(R)}$ is the phonon interfacial thermal conductance for the Pt(GGG)|YIG interface. In the following, we set $l_L / l_R \sim 1$ and take $l_R \sim 100$ nm [16].

In YIG, scattering processes among thermal magnons, which are governed by exchange interactions, occur on a much shorter time scale than magnon lifetime. Magnons are assumed to remain in a thermal distribution, which is then described by a magnon temperature $T_m(x)$ and an effective magnon chemical potential $\mu(x)$ [5,23] that parametrize the nonequilibrium distribution induced by the thermal bias. Treating transport semiclassically, the magnon spin- and heat-continuity equations read as [7]

$$\partial_t n + \partial_x j = -g_{n\mu}\mu - g_{nT}(T_m - T_p), \tag{2a}$$

$$\partial_t u + \partial_x q = -g_{uT}(T_m - T_p) - g_{u\mu}\mu, \tag{2b}$$

where n is the density of the thermal magnons and u is the energy density carried by them. The $g_{n\mu}$ and $g_{u\mu}$ coefficients account for the relaxation by the phononic environment of the magnons' spin and temperature, respectively. The cross terms g_{nT} and g_{uT} describe the generation or decay of spin accumulation by heating or cooling of magnons and vice versa and are related by the Onsager-Kelvin relation, i.e., $T_m\, g_{nT} = g_{u\mu}$. In the linear-response regime and neglecting magnon-phonon drag contributions $j,\ q \propto \partial_x T_p$ (restoring the phonon drag would simply rescale the bulk bias terms proportional to $\partial_x T_p$), the spin j, and heat q currents carried by the magnons can be written as

$$j = -\sigma\, \partial_x \mu - \zeta\, \partial_x T_m, \tag{3a}$$

$$q = -\kappa\, \partial_x T_m - \varrho\, \partial_x \mu, \tag{3b}$$

where σ, κ, ζ, and $\varrho = T_m \zeta$ are the bulk spin and heat conductivities and the intrinsic spin Seebeck and spin-Peltier coefficients, respectively.

Equations (2a) and (2b) must be determined consistently with the boundary conditions for spin and heat transport at the Pt|YIG and YIG|GGG interfaces. For Pt|YIG, at $x = 0$, the latter reads as

$$j = -G_L \mu + S_L \delta T_L + S_L (T_p - T_m), \tag{4a}$$

$$q = K_L \delta T_L + K_L (T_p - T_m) - \Pi_L \mu, \tag{4b}$$

where G_L, K_L, S_L, and $\Pi_L = T_m S_L$ are the interfacial magnon spin and thermal conductances and spin-Seebeck and spin-Peltier coefficients, respectively. Note that the spin current (4a) injected at the Pt|YIG interface is directly proportional to the measurable inverse spin-Hall voltage [24].

At the YIG|GGG interface, the spin flow is blocked as there are no spin carriers in the GGG substrate. Nevertheless, heat still can be transmitted via inelastic spin-preserving scattering processes between magnons and phonons. The corresponding boundary conditions at $x = d$ can be written as

$$j = 0, \tag{5a}$$

$$q = K_R\, \delta T_R - K_R (T_p - T_m). \tag{5b}$$

Here, K_R is the interfacial magnon heat conductance, which accounts for the processes leading to the energy exchange between magnons and phonons at the YIG|GGG interface. The interfacial magnon spin conductance G_R, the spin Seebeck S_R, and, consequently, the spin Peltier coefficient $\Pi_R = T_m S_R$ vanish.

Next we introduce the magnon energy relaxation length $\lambda_u = \sqrt{\kappa / g_{uT}}$ and the spin-diffusion length $\lambda_s = \sqrt{\sigma / g_{n\mu}}$, which parametrize the relaxation of the magnon temperature to the phonon temperature and the relaxation of the magnon chemical potential to its equilibrium (vanishing) value, respectively. Since the spin-preserving relaxation of magnon distribution towards the phonon temperature does not rely on relativistic spin-orbit interactions, the associated length scale λ_u can be taken to be much shorter than the spin-diffusion length λ_s [5,7,25], which here we set to $\lambda_s \sim 10\mu$m [3].

Based on the latter assumption, we identify two distinct transport regimes as functions of the thickness d of YIG. When the thickness is comparable or larger than the spin-diffusion length, i.e., $d \sim \lambda_s \gg \lambda_u$, we assume the transport to be dominated by the mechanisms leading to the relaxation of the

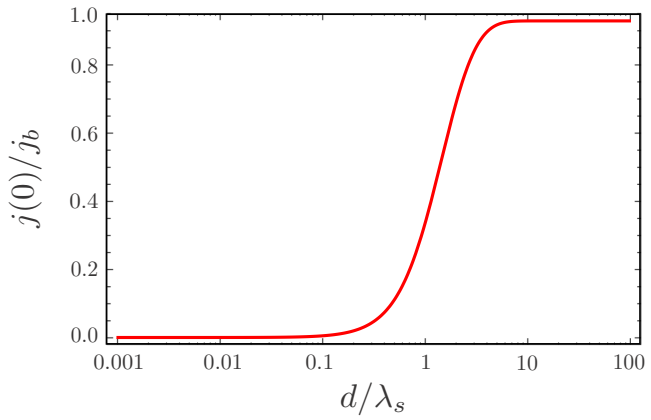

FIG. 4. Thickness dependence of the spin current $j(0)$ injected at the Pt|YIG interface in the far regime, i.e., where the thickness is represented on the scale of the magnon spin-diffusion length λ_s. Here, spin transport is dominated by the mechanisms leading to relaxation of the magnon chemical potential. The spin current is normalized by the thermal spin current in the bulk $j_b = -\zeta\, \partial_x\, T_p$.

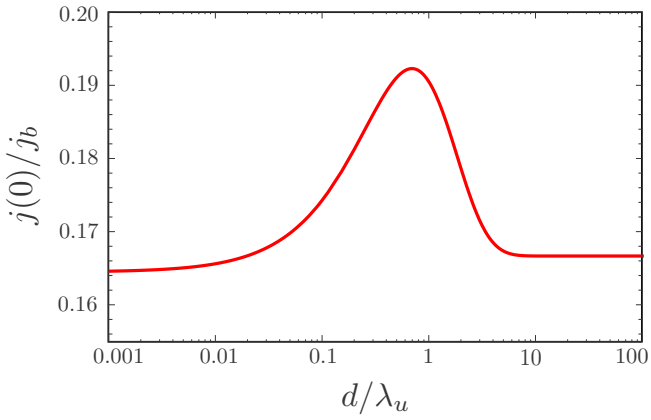

FIG. 5. Thickness dependence of the spin current $j(0)$ injected at the Pt|YIG interface in the near regime, i.e., where the thickness is represented on the scale of the magnon energy relaxation length λ_u. Here, the chemical-potential imbalance is disregarded, and the nonmonotonicity results from the interplay between the λ_u and the presence of cold magnons at the YIG|GGG interface. The spin current is normalized by the thermal spin current in the bulk $j_b = -\zeta\, \partial_x\, T_p$.

magnon chemical potential while setting $T_p = T_m$ throughout YIG [19]. As shown in Fig. 4, the corresponding contribution to the injected current at the Pt|YIG interface grows monotonically as a function of the YIG thickness, ultimately to saturate for large thicknesses. The underlying physical picture is clear. The temperature bias induces a chemical potential imbalance at the left interface. The corresponding magnon density increases with increasing sample thickness. However, when $d \gg \lambda_s$, magnons will decay—via non-spin-preserving interactions with the lattice—before reaching the left end of the sample, and the SSE signal will not increase further.

In the opposite regime, when $d \sim \lambda_u \ll \lambda_s$, the magnon-phonon temperature imbalance, $T_m - T_p$, becomes important. In order to illustrate the qualitative aspects arising due to its thickness dependence and the associated magnon flow, we switch to a simplified scenario, in which the chemical-potential imbalance is disregarded. In this case, the relaxation of the magnon temperature to the phonon temperature emerges as a driving mechanism for transport. In order to analyze the corresponding contribution to the injected spin current, we treat the magnon heat Kapitza length $\ell^*_{T,R} = \kappa/K_R$ at the YIG|GGG interface as a free parameter as there is no current estimate for interfacial thermal conductance K_R. Estimates for the other length scales can be found in the Supplemental Material [19]. The injected spin current exhibits a nonmonotonic behavior when $\ell^*_{T,R} \ll \ell^*_{T,L}, \lambda_u$, as shown in Fig. 5. To understand this result, recall that the magnon heat Kapitza length $\ell^*_{T,R}$ parametrizes the strength of spin-preserving inelastic interactions between magnons in YIG and phonons at GGG at the right interface; in other words, a short $\ell^*_{T,R}$ corresponds to an efficient thermalization process. As the phonon temperature in the GGG substrate $T_{p,L(R)}$ is lower than that in YIG, i.e., $\delta T_R > 0$, thermalization mechanisms between magnons in YIG and phonons in GGG lower the magnon temperature T_m near the YIG|GGG interface over a shorter time scale than the one governing the thermalization of the magnons and phonons in YIG. Hence, the right interface acts as a source of "cold" magnons, which contribute positively to the temperature imbalance in YIG $T_p - T_m$. However, when the sample thickness is larger than the temperature relaxation length λ_u, these magnons thermalize with phonons before reaching the left interface. Thus, for $d > \lambda_u$, the YIG|GGG interface no longer acts as an effective source for the magnon-phonon temperature imbalance in YIG, leading to the nonmonotonicity observed in Fig. 5. We suggest that this theoretical feature is related to our experimental observations and imply that the thickness at which the peak in SSR versus YIG thickness emerges is in direct correspondence with the magnon energy relaxation length in YIG, leading to an experimental estimate of the latter as $\lambda_u \sim 250$ nm.

Note that SSR data shown in Fig. 1 exhibits only a weak temperature dependence. This translates into a weak temperature dependence of the energy relaxation length λ_u. The spin diffusion length λ_s extracted in Refs. [26,27] is similarly rather insensitive to temperature variations. This appears quite surprising, as all these quantities are expected to scale strongly with temperature within simple transport theories [2,5,7], which is an issue that should be investigated in the future.

To summarize, our data and model suggest that the measured dependence of the SSR on the sample thickness reflects magnon spin- and heat-diffusion processes occurring on separate length scales. We show how a nonmonotonic feature in the signal observed at short thicknesses can emerge corresponding to the length scale parametrizing magnon-phonon thermalization mechanisms, and we offer an estimate for the latter, i.e., $\lambda_u \sim 250$ nm. Although a diffusive approach to the magnon heat transport qualitatively captures the newly observed feature, here we want to stress that our model represents a concept rather than a complete theory of transport at short thicknesses. Future work should address the nonequilibrium mechanisms operating over such length scales beyond the diffusive approximation rigorously.

This work was supported primarily by the Center for Emergent Materials, an NSF MRSEC, Grant No. DMR-1420451, the Army Research Office (ARO) MURI Grant No. W911NF-14-1-0016, and the U.S. Department of Energy (DOE), Office of Science, Basic Energy Sciences, Grant No. DE-SC0001304. Additional funding for the theoretical work is from the European Research Council, and the D-ITP consortium, a program of the Netherlands Organization for Scientific Research (NWO) that is supported by the Dutch Ministry of Education, Culture and Science (OCW).

[1] K. Uchida, H. Adachi, T. Ota, H. Nakayama, S. Maekawa, and E. Saitoh, Appl. Phys. Lett. **97**, 172505 (2010).
[2] S. Hoffman, K. Sato, and Y. Tserkovnyak, Phys. Rev. B **88**, 064408 (2013).
[3] L. J. Cornelissen, J. Liu, R. A. Duine, J. Ben Youssef, and B. J. van Wees, Nat. Phys. **11**, 1022 (2015).
[4] B. L. Giles, Z. Yang, J. S. Jamison, and R. C. Myers, Phys. Rev. B **92**, 224415 (2015).
[5] L. J. Cornelissen, K. J. H. Peters, G. E. W. Bauer, R. A. Duine, and B. J. van Wees, Phys. Rev. B **94**, 014412 (2016).
[6] D. J. Sanders and D. Walton, Phys. Rev. B **15**, 1489 (1977).
[7] B. Flebus, S. A. Bender, Y. Tserkovnyak, and R. A. Duine, Phys. Rev. Lett. **116**, 117201 (2016).
[8] J. Flipse, F. K. Dejene, D. Wagenaar, G. E. W. Bauer, J. Ben Youssef, and B. J. van Wees, Phys. Rev. Lett. **113**, 027601 (2014).
[9] M. Agrawal, V. I. Vasyuchka, A. A. Serga, A. D. Karenowska, G. A. Melkov, and B. Hillebrands, Phys. Rev. Lett. **111**, 107204 (2013).
[10] C. M. Jaworski, J. Yang, S. Mack, D. D. Awschalom, R. C. Myers, and J. P. Heremans, Phys. Rev. Lett. **106**, 186601 (2011).
[11] H. Adachi, K. Uchida, E. Saitoh, J. Ohe, S. Takahashi, and S. Maekawa, Appl. Phys. Lett. **97**, 252506 (2010).
[12] M. Agrawal, V. I. Vasyuchka, A. A. Serga, A. Kirihara, P. Pirro, T. Langner, M. B. Jungfleisch, A. V. Chumak, E. T. Papaioannou, and B. Hillebrands, Phys. Rev. B **89**, 224414 (2014).
[13] A. Kehlberger *et al.*, Phys. Rev. Lett. **115**, 096602 (2015).
[14] E.-J. Guo, J. Cramer, A. Kehlberger, C. A. Ferguson, D. A. MacLaren, G. Jakob, and M. Kläui, Phys. Rev. X **6**, 031012 (2016).
[15] J. Shan, L. J. Cornelissen, N. Vlietstra, J. Ben Youssef, T. Kuschel, R. A. Duine, and B. J. van Wees. Phys. Rev. B **94**, 174437 (2016).
[16] M. Schreier, A. Kamra, M. Weiler, J. Xiao, G. E. W. Bauer, R. Gross, and S. T. B. Goennenwein, Phys. Rev. B **88**, 094410 (2013).
[17] J. C. Gallagher *et al.*, Appl. Phys. Lett. **109**, 072401 (2016).
[18] C. L. Jermain, S. V. Aradhya, N. D. Reynolds, R. A. Buhrman, J. T. Brangham, M. R. Page, P. C. Hammel, F. Y. Yang, and D. C. Ralph, Phys. Rev. B **95**, 174411 (2017).
[19] See Supplemental Material at http://link.aps.org/supplemental/10.1103/PhysRevB.97.020408 for (a) the results of the main text but now plotted in the more conventional way as the ratio of the spin Seebeck signal divided by the temperature gradient rather than plotted as in the main text; (b) the sample magnetization data, used to characterize the quality of the samples; (c) the detailed algebraic derivation of the transport theory, the results of which are summarized in the main text.
[20] A. Prakash, J. Brangham, F. Yang, and J. P. Heremans, Phys. Rev. B **94**, 014427 (2016).
[21] S. R. Boona and J. P. Heremans, Phys. Rev. B **90**, 064421 (2014).
[22] A. Sola, P. Bougiatioti, M. Kuepferling, D. Meier, G. Reiss, M. Pasquale, T. Kuschel, and V. Basso, Sci. Rep. **7**, 46752 (2017).
[23] C. Du *et al.*, Science **357**, 195 (2017).
[24] J. Xiao, G. E. W. Bauer, K.-c. Uchida, E. Saitoh, and S. Maekawa, Phys. Rev. B **81**, 214418 (2010).
[25] B. Flebus, K. Shen, T. Kikkawa, K.-i. Uchida, Z. Qiu, E. Saitoh, R. A. Duine, and G. E. W. Bauer, Phys. Rev. B **95**, 144420 (2017).
[26] M. Sparks, *Ferromagnetic-Relaxation Theory* (McGraw-Hill, New York, 1964), p. 161.
[27] H. Maier-Flaig, S. Klingler, C. Dubs, O. Surzhenko, R. Gross, M. Weiler, H. Huebl, and S. T. B Goennenwein. Phys. Rev. B **95**, 214423 (2017).